

Correlation of Silicone Incorporation into Hybrid Acrylic Coatings with the Resulting Hydrophobic and Thermal Properties

Raquel Rodríguez,[†] Carolina de las Heras Alarcón,[‡] Piyasiri Ekanayake,^{*,§}
Peter J. McDonald,[‡] Joseph L. Keddie,[‡] María J. Barandiaran,[†] and José M. Asua^{*,†}

Institute for Polymer Materials POLYMAT and Grupo de Ingeniería Química, Departamento de Química Aplicada, Facultad de Ciencias Químicas, The University of the Basque Country, Centro Joxe Mari Korta, Avda Tolosa 72, 20018 Donostia-San Sebastián, Spain, and Department of Physics, Faculty of Engineering and Physical Sciences, University of Surrey, Guildford, Surrey GU2 7XH, U.K.

Received March 18, 2008; Revised Manuscript Received September 23, 2008

ABSTRACT: A series of high-solids hybrid silicone–acrylic latexes, with varying silicone concentrations and reactivities, was prepared via miniemulsion polymerization. The properties of the resulting coatings have been correlated with their structure and the extent of silicone grafting. The highest silicone incorporation was obtained with silicones containing two reactive vinyl groups polymerized by a semicontinuous method with a delayed addition of neat monomer. It was found that the amount of silicone grafted to the acrylic chains, *not* the overall total amount in the formulation, was the main factor affecting film properties. Hydrophobicity, water resistance, and thermal stability all increased with the amount of grafted silicone. Coatings that contained high levels of *nongrafted* silicone displayed separate submicrometer silicone phases and exhibited inferior properties. When silicone was incorporated into the acrylic particles, the total drying time of the coating was shorter, and the water distribution—as determined with magnetic resonance profiling—was more uniform, in comparison to an acrylic coating. A blend of a silicone emulsion and the acrylic latex displayed a nonuniform water distribution at later times with significantly slower drying—indicative of the formation of a “skin” layer consisting of coalesced silicone droplets. Thus, incorporation of the silicone within the acrylic particles offers clear advantages in the film formation process. These results indicate that the hybrid latex is superior for coatings in comparison to the acrylic or to blends of the acrylic with silicone.

Introduction

With a worldwide annual production in excess of 20 million metric tons, waterborne dispersed polymers are used in a wide range of applications including coatings, adhesives, additives for paper and textiles, leather treatment, impact modifiers for plastic matrixes, additives for construction materials, and synthetic rubber.¹ The rapid development of this industry has been driven by environmental concerns and governmental regulations to reduce the emissions of volatile organic compounds into the atmosphere. Waterborne polymers are a cleaner alternative to solvent-cast materials. Moreover, dispersed polymers offer unique properties, which meet a wide range of application needs, because of the ability to control structure at the nanoscale. The more advanced of these dispersed polymers are nanocomposite particles. These are high performance products, which present advantages with respect to more conventional products, because the properties of the constituent polymers can be combined in a synergistic way.

Silicone-modified acrylic latexes are particularly interesting materials, because they can potentially combine the advantages of both acrylics and polysiloxanes, while compensating for the limitations of each component. Acrylic latexes present good film-forming properties combined with good mechanical properties, and therefore are widely used in applications such as coatings and adhesives. However, acrylics usually suffer from poor thermal stability and poor water resistance, which is a problem for exterior coatings. On the other hand, silicone polymers present unique properties such as low surface energy, oil and chemical resistance, high flexibility, excellent thermal

stability, and resistance to outdoor weathering. However, unless they are cross-linked, silicones have very poor mechanical performance. A composite of an acrylic and a silicone has the potential to have the mechanical properties of an acrylic coupled with the thermal stability and water resistance of silicones, with each component overcoming the weakness of the other.

The synthesis route to produce a hybrid latex can influence the nanostructure of the particles and the film morphology and hence the properties of the resulting material. Several previous studies have focused on the production of core–shell particles by seeded emulsion polymerization of either acrylic (or styrene) monomers in the presence of siloxane seed² or siloxane onto the polyacrylate seed latex.³ For instance, Lin et al.² synthesized nanocomposite latex particles with a polydimethylsiloxane (PDMS) core and poly(methyl methacrylate-*co*-*n*-butyl acrylate) copolymer shell, as well as silicone/polyacrylate latexes compatibilized by introducing vinyl groups in the latex core. They observed a higher degree of hydrophobicity of the film when the compatibilizer was added, because of the multilobular morphology of the particles, with some PDMS domains between the polyacrylic hemispheres, in contrast to the pure PDMS core/acrylic shell in which the PDMS was fully encapsulated. Kan et al.⁴ observed that semicontinuous emulsion polymerization was an adequate process to obtain copolymer latexes of styrene–butyl acrylate and silicone. In their publication, they did not present the morphology of the particles, but they showed an increase in the water resistance and impact strength of the latex with increasing silicone content. On the other hand, the latexes with acrylic core and PDMS shell morphologies compatibilized by using a cross-linker³ showed water adsorption and hardness similar to those of cross-linked polysiloxane films, probably because the exterior of the particles mainly determines these properties. Silicone-grafted-butyl acrylate (BA)–styrene (St) copolymers were also produced by batch emulsion polymerization, obtaining more hydrophobic latex films than the

* To whom correspondence should be addressed. E-mail: jm.asua@ehu.es.

[†] The University of the Basque Country.

[‡] University of Surrey.

[§] Present address: Department of Physics, University of Peradeniya, Peradeniya, Sri Lanka.

Table 1. Formulations^a Used in the Polymerizations

code name	method	PDMS ^b (g)	PDMS type ^c	SA (g)	initiator (g)
BM0	batch	0	N/A	4	0.75 KPS
BM3	batch	3	DV	4	0.75 KPS
BM5	batch	5	DV	0	0.75 KPS
BM12	batch	12	DV	0	0.75 KPS
BM25	batch	25	DV	0	0.75 KPS
BM25N	batch	25	NR	0	0.75 KPS
BM25(20VP)	batch	25	MV	0	0.75 KPS
SM0	semicontinuous	0	N/A	4	0.5 (APS/SBS)
SM3	semicontinuous	3	DV	4	0.5 (APS/SBS)
SM12	semicontinuous	12	DV	0	0.5 (APS/SBS)
SM25	semicontinuous	25	DV	0	0.5 (APS/SBS)
SBS25	semicontinuous with shot	25	DV	0	0.5 (APS/SBS)

^a All formulations contain 1.8 g of Dowfax 2A1. ^b Mass corresponding to 100 g of monomer (MMA/BA/AA) at a ratio of 50:49:1. ^c N/A = not applicable; DV = divinyl; NR = nonreactive; MV = monovinyl.

corresponding poly(St-co-BA) latex films without silicone.⁵ Liu et al.⁶ synthesized, in a batch method, modified methyl methacrylate (MMA)–butyl acrylate–acrylic acid latexes containing different amounts of silicone (vinyltriethoxysilane) and observed that the incorporation of the silicone lowered the water adsorption and enhanced the thermal stability. However, immiscibility was greater as the silicone amount increased, due to the incompatibility between the hydrophobic silicone and the more hydrophilic monomers. A cross-linking agent would be necessary to compatibilize both phases.

Miniemulsion polymerization has emerged as a promising polymerization strategy for the synthesis of stable acrylic/silicone hybrid latexes, because monomer droplets are the main loci of particle formation, and water-insoluble compounds can be incorporated within the monomer droplets.⁷ Therefore, no additional cross-linkers are needed for compatibilization. Marcu et al.⁸ synthesized silicone/*n*-butyl acrylate stable latexes by batch miniemulsion polymerization, but properties of the films were not reported. Miniemulsion polymerization of MMA/BA with vinylsiloxane rubber was investigated by Yu et al., and the particle morphology and grafting were evaluated.⁹ However, the authors did not report on film properties. In summary, there has been good progress in the preparation of hybrid acrylic/silicone waterborne polymers, but the resulting structures have not been well correlated with resulting properties. In particular, there has been little study of the effect of silicone grafting to the second polymer on film properties, but rather the emphasis has been on the total amount of silicone contained within the hybrid material. Furthermore, with the exception of the work by Liu et al.,⁶ only low-solids-content latexes (below 20%) have previously been synthesized and analyzed. However, high-solids-content products are required for commercial applications. Their development is therefore essential for progress in applications.

This paper concerns high-solids-content silicone-modified acrylic latexes produced by miniemulsion polymerization, using both batch and semicontinuous processes. In the present work, we have correlated the amount and type of silicones and the method of miniemulsion polymerization with the hydrophobicity, water repellency, and thermal resistance of the resulting coating. In particular, we consider the effect of the amount of silicone chemically grafted to the acrylic *rather* than merely the *total* amount of silicone in the formulation. We correlate the properties of the coatings with their phase distribution and nanostructure.

Moreover, the film formation process of waterborne polymer colloids is important because of its impact on film properties. In particular, nonuniformity of water during the drying process can cause “skin formation” in which a coalesced surface develops over a wet interior.¹⁰ Consequently, water loss from further evaporation is severely slowed down.^{11,12} Water trapped within polymer films (because of skin formation) can be

detrimental to their cohesive strength and adhesion.¹³ It is predicted¹¹ that colloidal polymers will create a skin layer when they are film-formed at temperatures well above their glass transition temperature (T_g), and this is the case for silicones at room temperature ($T_g = -127\text{ }^\circ\text{C}$). In fact, previous research has found that silicone emulsions are particularly prone to such skin formation.¹⁴ Hence, in this work the influence of the introduction of silicone on the drying uniformity of the acrylic films was investigated. A comparison was made between the drying of the hybrid latex and the drying of a blend of acrylic latex with silicone emulsion. Additionally, some properties—including wettability and stain resistance—will be affected by the vertical distribution (i.e., perpendicular to the substrate) of the silicone in the final film; hence this characteristic was also investigated.

Experimental Details

Materials. Technical grade monomers methyl methacrylate (MMA) and butyl acrylate (BA), supplied by Quimidroga, and acrylic acid (AA, Aldrich) were used without purification. Divinyl-terminated polydimethylsiloxane (DV-PDMS, Aldrich), monovinyl-terminated polydimethylsiloxane (MV-PDMS, Wacker), and non-reactive polydimethylsiloxane (N-PDMS, Wacker) were used as resins; stearyl acrylate (SA, Aldrich) was used as a costabilizer; Dowfax 2A1 (alkyldiphenyl oxide disulfonate, Dow Chemical) was used as the surfactant. Potassium persulfate (KPS, Panreac) or a 1:1 molar ratio of ammonium persulfate (APS, Panreac) and sodium metabisulfite (SBS, Aldrich) was used as redox initiator system. Distilled water was used in all polymerizations.

Polymerization Procedures. The high-solids-content (50 wt % organic phase) silicone/acrylic hybrid latexes were synthesized by miniemulsion polymerization, in either batch or semicontinuous processes. Batch polymerizations were carried out in a 1 L glass reactor equipped with reflux condenser, stirrer, sampling device, and nitrogen inlet. The reaction temperature was maintained constant at 70 °C by controlling the temperature of the fluid in the jacket by means of a thermostatic bath and a heat exchanger. The miniemulsion was added to the reactor and kept under a nitrogen atmosphere using a flow rate of 12–15 mL/min. The initiator was injected when the reaction temperature was reached. The polymerizations carried out in batch are designated hereafter by “BM”.

Semicontinuous polymerizations were carried out in the same reactor setup as the batch polymerizations. Two different strategies were explored. In the first one, 33 wt % miniemulsion (50 wt % organic phase) was used as the initial charge, and it was allowed to polymerize over 1 h. Then, the rest of the miniemulsion and the initiator system were fed over a period of 4 h. This semicontinuous method of polymerization is designated by “SM”. The second semicontinuous strategy differed from the first one in that a fraction of monomer was fed as a miniemulsion over 210 min, and then the remaining monomer was fed as neat monomer over 1 h. This strategy is designated by “SBS”. All the reactions were carried out at 70 °C. A summary of all formulations is presented in Table 1.

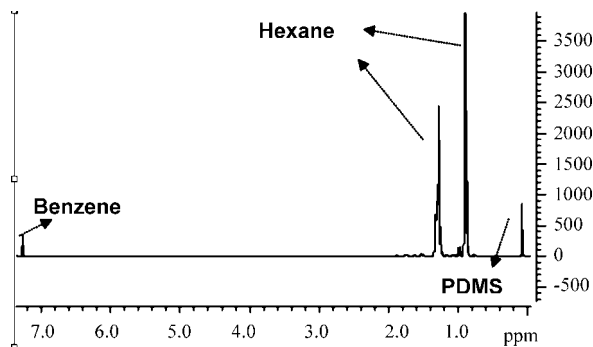


Figure 1. ^1H NMR spectrum of the product extracted from latex BM25, showing a peak attributed to PDMS.

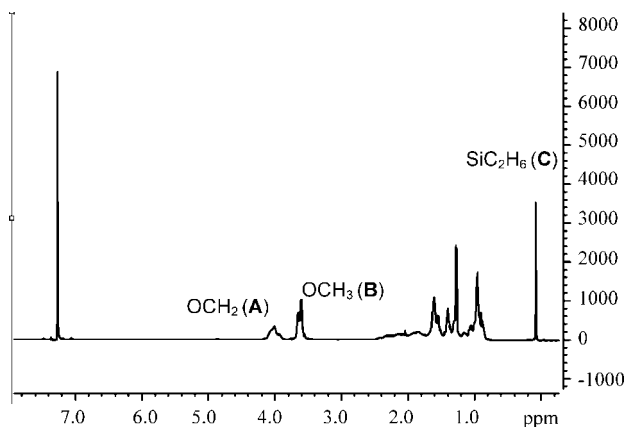


Figure 2. ^1H NMR spectrum of BM25 after selective extraction, showing peaks attributed to the acrylic copolymer (A and B) and to PDMS (C).

The number in the code names for the latexes represents the mass of PDMS in grams per 100 g of acrylic monomer.

In order to check the extent of PDMS homopolymerization, a batch solution homopolymerization of PDMS was carried out at 70 °C in *p*-xylene, using AIBN as the initiator. No polymerization was observed in 9 h.

The drying of films of blended acrylic latex (SM0) and a PDMS emulsion was studied with magnetic resonance profiling experiments. The emulsion was prepared by ultrasonication in a Branson Sonifier 450 of the N-PDMS (125 g) in water (125 g) with 1.8 g of Dowfax 2A1 surfactant.

Characterization. Quantification of Grafted Silicone. The amount of chemically bound PDMS in the hybrid latex particles was determined by ^1H NMR spectroscopy (Bruker Avance 500 MHz) after selective Soxhlet extraction of the unreacted PDMS with hexane.

The procedure to extract the unreacted PDMS was as follows. First, the latex, in which hydroquinone had been added to avoid further reactions during the extraction, was coagulated using a solution of CaCl_2 (0.45 g of CaCl_2 in 50 g of H_2O) at 60 °C. The coagulum thus obtained was dried in a ventilated oven overnight. The dry latex was placed into a cartridge inside a Soxhlet vessel with boiling hexane over 24 h. Then, the ^1H NMR spectrum of the solution was obtained.

Transmission Electron Microscopy (TEM). TEM images were obtained with an Hitachi 7000FA microscope. The latexes were stained by adding small amounts of phototungstic acid. The particles were cast on copper grids covered with polyvinylformal (Formvar R) and dried under a UV lamp in order to avoid film formation. Six different regions of the same sample were analyzed to ensure that the images were representative.

Atomic Force Microscopy (AFM). All AFM measurements were performed with an instrument (NTEGRA, NT-MDT, Moscow, Russia) operating in intermittent contact ("tapping") mode using a

silicon cantilever (NT-MDT). The resonant frequencies of the cantilevers ranged between 115 and 150 kHz, and their nominal spring constant was 10 N/m. The "free" amplitude of the cantilever, A_0 (corresponding to oscillation in air), was fixed at 323 nm. The set-point amplitude, A_{sp} (corresponding to the amplitude when the tip is in contact with the sample surface), was kept at 108 nm, thus making the set-point ratio, A_{sp}/A_0 , equal to 0.3 for all measurements. Films were cast on PET film and allowed to dry overnight at a temperature of 22 ± 1 °C and a relative humidity of $55 \pm 1\%$. The dried films for AFM analysis were about 20 μm thick. Three different regions of the films were analyzed.

Magnetic Resonance (MR) Profiling. The distribution of water during the drying of the latex films was investigated using MR profiling. The experiments employed a permanent magnet, called GARField (Gradient At Right-angles to the Field),^{15–17} which was specifically designed to determine profiles of thin layers in the direction normal to the surface. Wet films (ca. 500 μm thick) were cast onto clean glass coverslips (2 cm \times 2 cm) and immediately placed in the magnet at a position corresponding to a magnetic field strength of 0.7 T and a field gradient strength of 17.5 T m⁻¹. Signals were obtained using a quadrature echo sequence¹⁸ $(90_x - \tau - 90_y - \tau - \text{echo} - \tau)_n$ for $n = 32$ echoes and a pulse gap of $\tau = 95$ μs . To obtain a profile, the echoes were Fourier transformed and then summed, thus giving an NMR signal intensity profile as a function of vertical position. The NMR intensity is a fair measure of the water content that can be calibrated from the time-zero data with a known, uniform concentration. The pixel resolution in these experiments was about 10 μm . To correct for the sensitivity decline over the film thickness, profile intensities were normalized by an elastomer standard. Films were dried under static air at a temperature about 25 °C.

Film Formation. Films with a wet thickness of 120 μm were cast on a glass substrate and dried for 1 day at an approximate temperature of 23 °C and relative humidity of 60%. These films were used for subsequent measurements of contact angle, water uptake, and thermal resistance.

The rates of water loss were determined for selected films by a gravimetric method. Films (with an initial thickness of approximately 110 μm) were cast on clean glass plates (6 cm \times 6 cm area) of known mass. The mass of the wet film in static air at a temperature of 22 °C was measured on a digital balance as a function of drying time. From the initial linear region of plots of water mass as a function of time, values of the evaporation rate (in units of mass per unit area per unit time) were calculated.

Contact Angle Measurements. The contact angle of water on the film was measured using an OCA 20 Dataphysic tensiometer. The contact angles were measured at both the air/film and film/substrate interfaces (after delamination).

Water Uptake. Water uptake was measured by immersing 6 cm² films in water and calculating the relative weight change. At intervals of 24 h, over a period of 1 week, the films were withdrawn from the water and weighed after shaking off any free water. Three samples of each film were used, and the average value was calculated. The error of the measurement was about 5%.

Thermal Stability. Thermogravimetric analysis (TGA) was carried out in a TGA 2950/Q500 (TA instruments), with film samples weighing 5 mg. The temperature ranged from 20 to 600 °C, and the heating rate was 10 °C/min in a nitrogen flow rate of 75 mL/min.

Results and Discussion

Silicone Grafting. Figure 1 shows the ^1H NMR spectrum of the product extracted from the sample BM25. It can be seen that no peaks corresponding to the acrylic polymer appeared, which indicates that only the free PDMS was dissolved. In addition, no peaks in the region of the double bonds were observed, likely because the intensity of these peaks was small. The peak at $\delta = 7.15$ ppm corresponds to benzene, which was used as internal patron because it does not interfere with the PDMS assignment peaks.

Table 2. Validation of the Selective Extraction Procedure

	PDMS _{unreacted} from ¹ H NMR		PDMS _{reacted} from ¹ H NMR		total PDMS by ¹ H NMR		total PDMS added in formulation (g)
	g	%	g	%	g	%	
BM3	0.18	2.6	7.42	97.4	7.60	97.3	7.81
BM25	39.83	24.2	12.70	75.8	52.53	97.5	53.87

Table 3. Extent of PDMS Grafting in the Various Polymerizations

code name	total PDMS used ^a (g)	unreacted PDMS ^a (g)	grafted PDMS ^a (g)	grafted PDMS (wt % of total PDMS)
BM3	3	0.09	2.91	97
BM5	5	0.1	4.9	98
BM12	12	7.7	4.3	36
BM25	25	19.2	5.8	23
SM3	3.0	0	3	100
SM12	12	5.4	6.6	55
SM25	25	14.5	10.5	42
SBS25	25	5	20	80
BM25(20VP)	25	21.7	3.3	13

^a With respect to 100 g of acrylic monomers.

Therefore, to quantify the amount of PDMS in the hexane solution, the signal of the methyl groups of the PDMS ($\delta = 0.2$ ppm) was considered. A calibration curve was constructed from ¹H NMR spectra of hexane solutions containing different PDMS concentrations.

On the other hand, the amount of PDMS remaining in the polymer was quantified from the ¹H NMR spectra of the nonextracted material. In Figure 2, area A is proportional to the two aliphatic protons of the OCH₂ group of BA, area B is proportional to the three aliphatic protons of the OCH₃ group of MMA, and area C is proportional to the six aliphatic protons of the two CH₃ groups of PDMS.

To validate the procedure, a selective extraction of two different samples was performed (BM3 and BM25). The procedure explained above was followed, and the extracted solution and the coagulated polymer after the extraction were analyzed by ¹H NMR spectroscopy, which allowed the calculation of the amount of unreacted and reacted PDMS, respectively. Table 2 shows that there was a good agreement between the total amount of PDMS determined by ¹H NMR spectroscopy and the known amount in the formulation.

Table 3 presents measurements of the amounts of PDMS incorporated in the various polymerizations. As the amount of PDMS was increased, a lower percentage of it was grafted to the acrylic. There is always a greater amount of grafting achieved in the semicontinuous method in comparison to the batch method. At the highest PDMS contents of 25 wt % on the acrylic monomer, the semicontinuous method with neat monomer addition (SBS25) yielded the greatest amount of silicone grafting.

Drying Rates and Water Distribution. Gravimetric measurements were used to compare the water evaporation rate, E , for three different coatings: acrylic copolymer (SM0), a hybrid latex containing 25% PDMS (SM25), and a blend of the acrylic (SM0) with 11 wt % PDMS emulsion. During the initial period when the evaporation rates were relatively constant, the hybrid latex dried fastest with $E = 4.2 \times 10^{-5}$ g cm⁻² min⁻¹ compared to the acrylic with $E = 3.5 \times 10^{-5}$ g cm⁻² min⁻¹. (Note that the uncertainty on these measurements is ± 0.1 g cm⁻² min⁻¹.) The water evaporation rate for the blend of the acrylic and the PDMS emulsion was slightly slower with $E = 3.1 \times 10^{-5}$ g cm⁻² min⁻¹. The slower water loss rates could be explained by the partial coalescence of particles near the film surface.

Analysis of the slowing down of the water loss rate has been used elsewhere¹⁹ to infer information on the water distribution in drying colloidal films. In this work, a direct measurement, GARField MR profiling, was used to probe the distribution of

water in the vertical direction throughout the entire drying process for latex films prepared by the semicontinuous polymerization process. Representative profiles, obtained at successive times throughout the film formation process, are presented in Figure 3. In all profiles, the film's air interface is represented on the right side of the profile, and the film-substrate interface is on the left side. The third axis shows the time measured from the start of the first profile. The NMR intensity is proportional to the concentration of *mobile* ¹H in the drying films.^{15,17} This means that as the water evaporates, and the water concentration decreases, the signal intensity (vertical axis) and film thickness (horizontal axis) both decrease.

No NMR signal is obtained in the profiling technique from ¹H in chemical groups with low molecular mobilities, as indicated by a low spin-spin relaxation time, T_2 . The acrylic copolymer has a T_2 of 60 μ s, according to measurements from a dry SM0 film, and so it does not yield a significant NMR signal in our experiments. When the acrylic film is fully dry, the profile intensity goes to zero.

The profiles in Figure 3 reveal significant differences in the water distribution in an acrylic copolymer film (SM0) in comparison to the hybrid latex film containing 25 wt % PDMS on the acrylic (SM25) and to a physical blend of the acrylic latex with a PDMS emulsion with either 25 wt % or 11 wt % PDMS on the acrylic. The profiles for the acrylic copolymer (SM0 in Figure 3a) show that a step in the NMR signal intensity develops early on in the drying process and persists to the later stage (about 55 min). Only water—and not the polymer—contributes to the signal. This step in the signal intensity corresponds to a step in the water concentration. A layer with lower water concentration develops at the top of the film and increases in thickness over time. This layer is attributed to the accumulation and packing of particles near the top of the SM0 film. After about 55 min the nonuniformity disappears. It is likely that the particles have now packed together throughout the depth of the film, so there is no longer a more dilute layer near the bottom of the film. The NMR signal disappears after about 80 min, indicating that the mobile water molecules have left the film. The film is dry.

The development of the water distribution in films of the hybrid acrylic/silicone latex (SM25) is quite different (Figure 3b). The distribution of the water profile is much more uniform through the depth of the film. No abrupt steps are observed in the intensity profiles. After 55 min, there are no further changes in the signal, indicating that all mobile water has left the film. The constant NMR intensity remaining beyond 55 min is attributed to the mobile ¹H in the liquidlike PDMS within the particles. The fact that this PDMS component yields an NMR signal indicates that the chemical grafting does not inhibit its molecular mobility.

Note that if the addition of PDMS had lowered the viscosity of the particles significantly, then particle coalescence in the wet state and the development of a skin layer would be expected from current models of film formation.^{10,11} Instead, there is no evidence from the profiles for skin formation or nonuniform water distribution. The shorter observed time for the complete water loss from the hybrid film is consistent with the gravimetric measurements.

The profiles for the film cast from the physical blends of acrylic and PDMS (Figure 3c,d) are significantly different from those for the plain acrylic. In a film containing 11 wt % PDMS

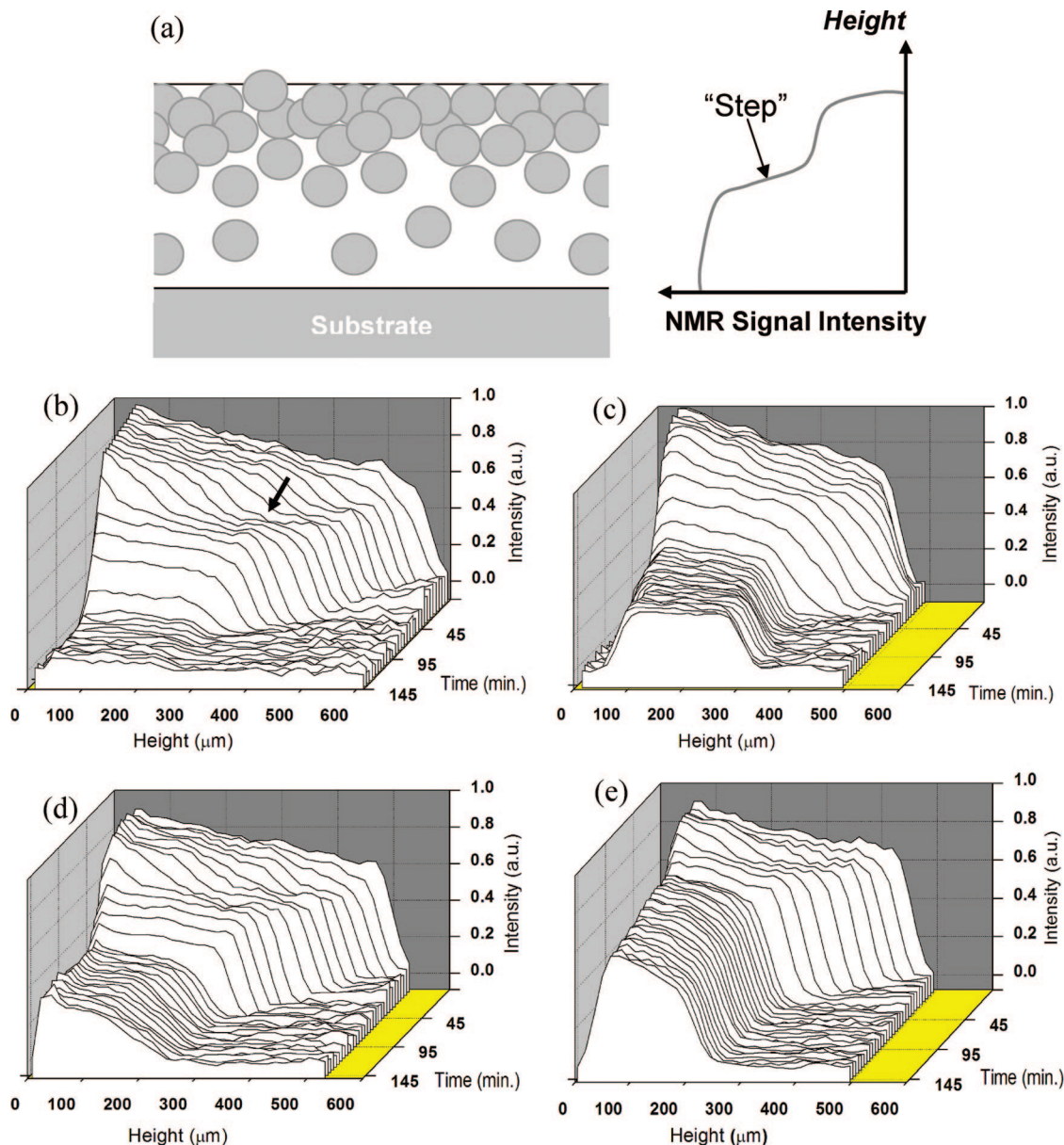


Figure 3. (a) Sketch of particle packing at the surface of a drying latex film, and illustration of the corresponding GARField profile. The profile has been drawn so that it corresponds with the film structure. Experimental GARField profiles obtained over time during the drying of latex prepared by the semicontinuous method with various compositions: (b) acrylic copolymer latex (SM0), (c) 25 wt % PDMS on the acrylic monomer (SM25), (d) physical blend of acrylic copolymer and 11 wt % PDMS emulsion, and (e) physical blend of acrylic copolymer and 25 wt % PDMS emulsion. The profiles are rotated 90° in comparison to the sketch: the NMR signal intensity is plotted as a function of vertical position in the film. The third axis shows times up to 150 min. The arrow in (b) points to a step in the NMR signal intensity in one of the profiles obtained at time of approximately 40 min.

(Figure 3c), a step in the water concentration indicates that there is particle packing near the film surface between times of 15 and 45 min. At a later time of 70 min, a shallow concentration gradient develops and persists over the times shown (up to 150 min). The very slow decrease in signal intensity over time, as observed in the MR profiles, is attributed to the gradual loss of water in a film of packed, deformed particles. The profiles obtained from the blend containing 25 wt % PDMS (Figure 3d) follow a broadly similar pattern. There is evidence for particle packing near the film surface at early time and a gradual loss of signal over time. When compared to the profiles from the SM25 hybrid (Figure 3b) of nominally the same overall composition, the water distribution is less uniform at the earlier times, and the signal decrease over time (related to the rate of water loss) is slower.

A calculation of the zero moment of statistics²⁰ provides the area under the profile, which is proportional to the concentration

of mobile water in the film, and can thereby provide information on the drying kinetics with good sensitivity over long periods of time. The area under the profiles was measured above a lower threshold value in order to eliminate any contribution from noise in the profile.

The plots of the time dependence of the zero moments in Figure 4 can be used to compare the rates of water loss for the four films. The slopes of the plots over the first 80 min show that the acrylic/silicone hybrid (SM25) film dries faster than the acrylic (SM0) and the two physical blend films. The zero moment for both the acrylic and the hybrid films is seen to become constant beyond times of about 100 min, indicating that drying is complete. There is no evidence for trapped water in these films.

Figure 4 highlights how very differently the physical blend films dry in comparison to the others. In the 25 wt % PDMS blend, there is a slowdown in the water loss after about 50 min

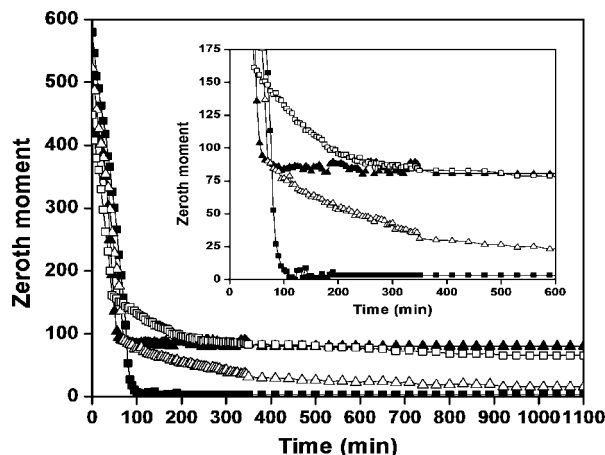


Figure 4. Comparison of GARField data for the acrylic copolymer (SM0, filled squares), 25 wt % PDMS on the acrylic monomer (SM25, filled triangles), and the physical blends of acrylic and 11 wt % PDMS (open triangles) and acrylic and 25 wt % PDMS (open squares). The zero moment is shown as a function of time up to 1100 min for the same four compositions. The inset shows the same data between 0 and 600 min.

of drying, which could be attributed to a partially coalesced surface layer. The water loss rate decreases a second time at about 200 min. Thereafter, until about 800 min, there is an exceedingly slow rate of water loss, which is consistent with a film in which the surface is sealed closed by a coalesced surface layer. The water loss in the blend film containing 11 wt % PDMS follows a similar pattern, although the second slowdown in water loss is observed at a later time of ca. 350 min. (Note that the zero-moment value for this last sample reaches a plateau at a rather low value. There are two explanations. One is that the molecular mobility of the PDMS is somewhat restricted, resulting in a lower NMR signal. A second explanation is that the zero moments have been calculated above a threshold value, such that the values are lowered. The contributions from these two effects cannot be disentangled.)

In summary of these observations, it is concluded that there is a stark difference between the drying pattern in the hybrid and the blend films. When PDMS is grafted within the acrylic latex particles, drying is relatively fast, and there is no evidence for skin formation or water entrapment. Skin formation is attributed to particle coalescence in films that dry nonuniformly.^{11,21} Hence, particle coalescence is not apparently provoked by the inclusion of PDMS in the hybrid particles. On the other hand, when separate PDMS droplets exist in the film, the drying is severely slowed. A likely explanation is that the PDMS droplets partially coalesce to create a barrier to the water transport. An advantage of the hybrid latex is that the PDMS is incorporated into the particles without encouraging particle coalescence.

Moreover, the faster drying in the hybrid latex (SM25) in comparison to the pure acrylic copolymer (SM0) can be attributed to greater hydrophobicity in the hybrid particles, which is investigated in later sections of this paper. Dewetting of the SM25 particles by water could be aiding the drying when the particles have packed into a film, whereas more hydrophilic boundaries in the SM0 latex could be retaining water, thereby reducing the water loss rate.

Distribution of PDMS in Films. With its very low T_g of -127°C , PDMS is liquidlike at room temperature. The T_2 relaxation time of pure PDMS was measured to be 160 ms, which is sufficiently high to yield an NMR signal. In our experiments, an NMR signal was obtained from dry hybrid films that contained PDMS. This result indicates that the PDMS

retains a significant molecular mobility, even when confined within the dry hybrid coating. The GARField profiles revealed a uniform concentration of PDMS vertically in the films, indicating that there was no phase separation over the length scale that is resolved by the technique: ca. $10\ \mu\text{m}$.

In an attempt to induce phase separation, films of the hybrid latex prepared by the batch method and containing 25 wt % PDMS on the acrylic (BM25) were heated at 150°C in a vacuum for 6 h. It was speculated that there could be some coarsening of the structure when the molecular mobility of the acrylic phase was greater. After this heat treatment, there was a decrease in the NMR signal, which is attributed to water loss. However, there was no evidence for phase separation of the PDMS and the acrylic. It is concluded that the film structure, with a uniform distribution of silicone, is robust.

Particle Structure and Film Morphology. TEM analysis of the individual hybrid particles prepared by the batch method using divinyl-PDMS (BM25) found evidence that some—but certainly not all—particles had an acrylic shell encapsulating a core that is enriched in PDMS (Figure 5a). In these images, the dark component is attributed to PDMS and the lighter component is attributed to the acrylic copolymer. In some particles, the boundaries between the shell and core were much less distinct, suggesting that there was greater mixing of the silicone and acrylic at the molecular level. This particular latex had an average of 23 wt % PDMS grafted to the acrylic copolymer, according to the NMR spectroscopy analysis. The structure observed in the TEM images is interpreted as having a core comprised of the nongrafted PDMS with the shell consisting primarily of acrylic copolymer with grafted PDMS. A similar variety of structures was found for the latex particles prepared by the semicontinuous process (Figure 5c,d), with some particles having a uniform structure while others had a core-shell structure. In contrast, nearly every one of the particles prepared with the nonreactive PDMS (BM25N) presented a clear and distinct nongrafted PDMS-rich core morphology with a fully encapsulating acrylic shell (Figure 5b). There was less variability in the particle structure in comparison to the particles containing reactive PDMS.

AFM analysis was carried out on films cast from these latexes to determine if the particle structure was preserved after film formation. The AFM phase contrast images from films of the BM25 latex (Figure 6a) provide evidence that particle identity is indeed retained. There is evidence for two components within the film. A few particles are observed to have a core-shell structure in which the core appears darker in the phase image. This contrast in the phase image indicates that there is more energy dissipation in the particle cores, which is what is expected for a more viscous silicone within a more elastic acrylic-rich shell.²² Our interpretation of the image is that in some particles the shell is sufficiently thin to enable the AFM tip to detect the core.

In a film cast from a hybrid latex using nonreactive PDMS (BM25N), in which none of the silicone can be grafted to the acrylic copolymer, AFM analysis reveals that a greater fraction of the particles exhibits a distinct core-shell structure (Figure 6b), in accordance with what is observed by TEM (Figure 5b). This structure is consistent with having no grafting between the acrylic and the silicone such that there are two separate phases. In some particles, the shell is likely to be thicker, so that the AFM tip does not penetrate the shell to detect the silicone core. Figure 6c shows a much more homogeneous film structure obtained from a hybrid latex (SM25) in which a greater PDMS fraction (42 wt %) is grafted to the acrylic. In this case, with a relatively low fraction of nongrafted silicone, the shell comprised of silicone grafted to acrylic is presumably much thicker, and there is greater mixing of the silicone and acrylic

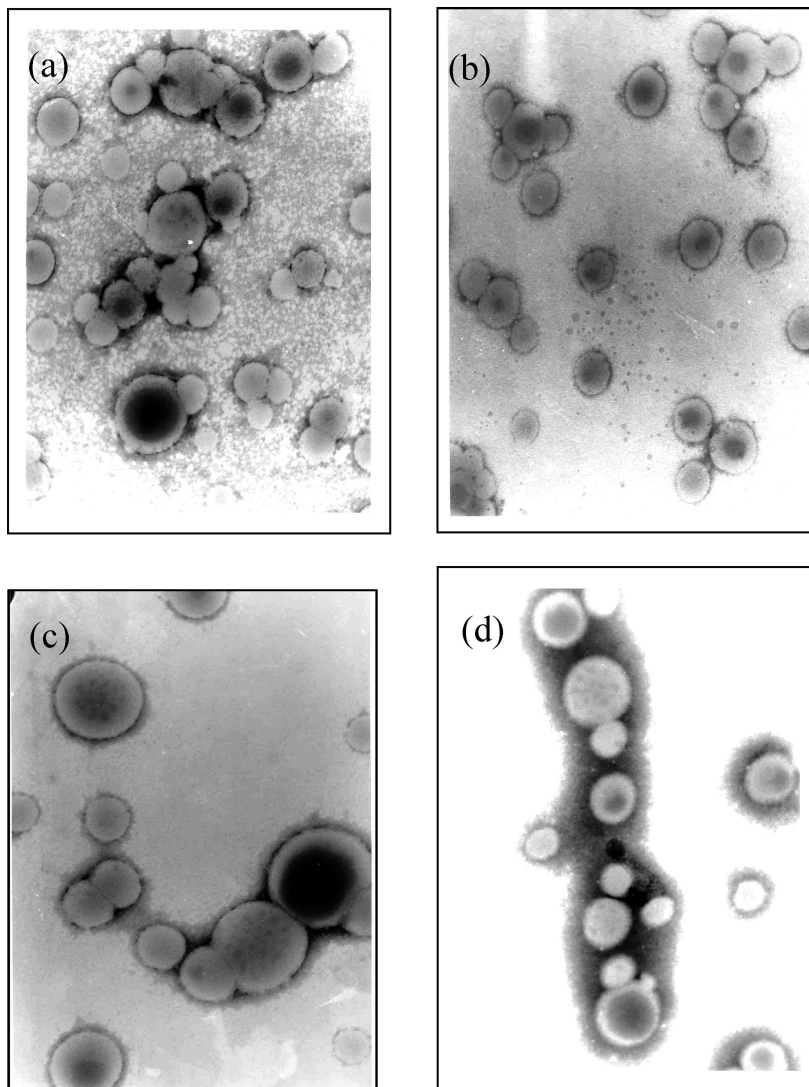


Figure 5. TEM images of hybrid silicone–acrylic latexes containing 25 wt % PDMS on the acrylic, prepared by the batch process using (a) DV-PDMS (BM25) and (b) nonreactive PDMS (BM25N) and by the semicontinuous process using DV-PDMS (c) miniemulsion feeding (SM25) and (d) net monomer feeding (SBS25).

at the molecular level. The AFM image of SBS25 (Figure 6d) shows a very homogeneous nanostructure.

Film Properties. In order to study the films' hydrophobicity, the water contact angle and water uptake were determined.

Contact Angle Measurements. Latex films with differing PDMS concentrations were cast on glass substrates. The films were peeled and rinsed with water to eliminate any surfactant migrated to the surfaces,²³ and the contact angles of both interfaces, air–film and film–substrate, were measured.

Figure 7a shows that, for the batch latexes (BM0, BM3, BM5, BM12 and BM25), the water contact angle increased with PDMS content up to 5 wt % (on the mass of the acrylic). Further increases in the PDMS content only led to marginal increases in contact angle on either of the interfaces. The latexes prepared by semicontinuous polymerization (SM0, SM3, SM12, and SM25) showed a similar behavior (Figure 7b). Moreover, almost no differences between air–film and film–substrate interfaces were observed, most likely because of the homogeneous distribution of the PDMS throughout the film, which is in accordance with the MR observation.

It is proposed that for the batch latexes the reason for the marginal increase in contact angle after 5 wt % PDMS was that a large fraction of the unreacted PDMS accumulated in the core of the polymer particles (as indicated by TEM and AFM

analyses in Figures 5 and 6), and hence it did not have much effect on surface properties. On the other hand, the reacted PDMS is expected to have access to the surface of the particle and, hence, it contributed to the interfacial properties of the coating; i.e., it was probably responsible for the increase in the water contact angle. The limiting value of the contact angle corresponds well with the fact that the amount of PDMS grafted into the copolymer did not increase substantially by increasing the PDMS content in the formulation (Table 3).

However, for the semicontinuous process the contact angle also showed small increases for larger amounts of PDMS (Figure 7b) whereas the amount of grafted PDMS clearly increased.

In order to investigate further the effect of the PDMS incorporation, the hydrophobicities of latexes containing 25 wt % monovinyl-terminated PDMS (BM25(20VP)) and nonreactive PDMS (BM25N) can be compared to those prepared with DV-PDMS. As shown in Table 3, the amount of PDMS grafting to the acrylic varies depending on the type of PDMS and on the method of polymerization (batch versus semicontinuous). Figure 8 compares the contact angles of the films cast with the latexes all containing 25 wt % PDMS. It is observed that the contact angles increase with the extent of grafting of PDMS to the acrylic polymer. The use of semicontinuous processes that led to a higher incorporation of the PDMS (Table 3) resulted in a

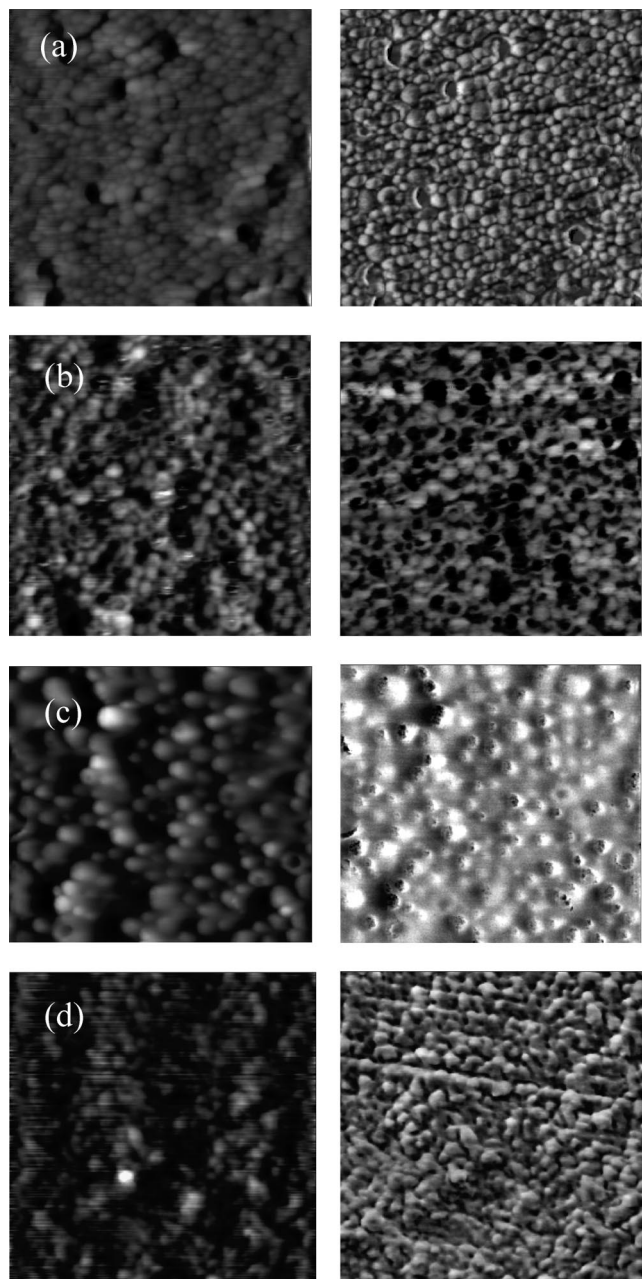


Figure 6. AFM images (height on left and phase contrast on right) of coatings cast from hybrid silicone-acrylic latex containing 25 wt % PDMS on the acrylic, prepared by the batch method using (a) divinyl PDMS (BM25) and (b) nonreactive PDMS (BM25N) and by the semicontinuous process using DV-PDMS (c) miniemulsion feeding (SM25) and (d) net monomer feeding (SBS25). All images are $2\ \mu\text{m} \times 2\ \mu\text{m}$.

higher contact angle (corresponding to a more hydrophobic coating surface). On the other hand, latex coatings made using nonreactive PDMS, in which the PDMS is believed to be encapsulated within the core of the particles, has a contact angle of 86° , which is higher than what was found for the neat acrylic ($\sim 70^\circ$). One explanation is that some PDMS has emerged from the particles and covered the film surface, but this layer is too thin to be resolved by MR profiling. Some of the contrast observed in the AFM phase image shown in Figure 5b could be attributed to free PDMS at the surface.

Moreover, it can be seen in Figure 8 that the increase in contact angle showed a saturation effect at high amounts of grafted PDMS. The contact angle on pure silicone is around 100° .²⁴ Therefore, it can be concluded that above a certain

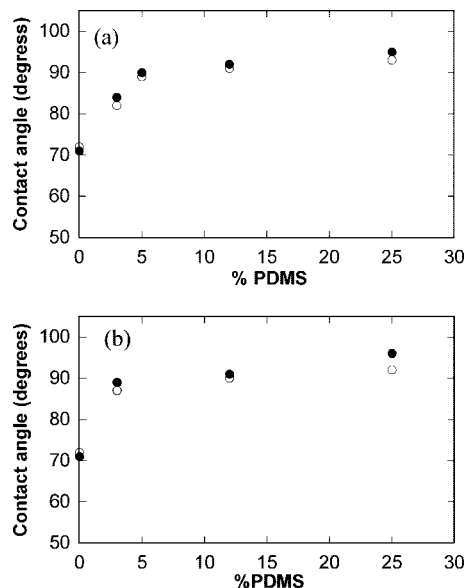


Figure 7. Effect of PDMS content on water contact angle on the (●) air-film and (○) film-substrate interfaces for latexes produced by miniemulsion polymerization in (a) batch and (b) semicontinuous (miniemulsion feeding) methods. The PDMS content is expressed as a mass percentage of the monomer mass.

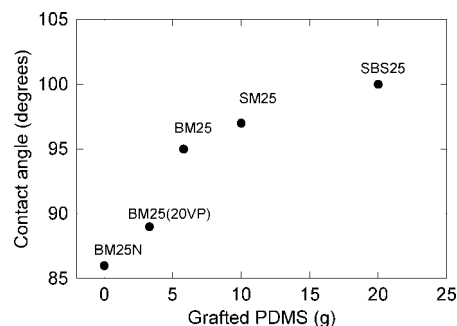


Figure 8. Water contact angle on hybrid silicone-acrylic coatings as a function of amount of PDMS grafting to the acrylic. Each coating contains 25 g of PDMS/100 g of acrylic.

grafting value there is no significant effect on the hydrophobicity of the film.

Water Uptake. Figure 9 shows that water uptake decreased as the PDMS content increased in both batch (BM) and semicontinuous with miniemulsion feeding (SM) polymerizations. In addition, the semicontinuous product had a lower water uptake in comparison to the BM coatings. Water uptake is defined here as the weight of water absorbed by 100 units of the weight of the total hybrid polymer (acrylic and silicone). As PDMS was not expected to absorb a significant level of water, it might be argued that the decrease with increasing silicone content was due merely to the amount of PDMS in the system, and that the water uptake of acrylic polymer itself was not affected.

This interpretation was tested with further analysis. Figure 10 presents the water uptake calculated with reference to the acrylic polymer in the latex (not the total polymer weight). It can be seen that, for the batch process, PDMS did not significantly affect the water uptake of the acrylic polymer. On the other hand, the presence of PDMS reduced the water uptake of the films cast with latexes obtained from the semicontinuous process, probably because of the better incorporation into the acrylic chains.

Thermal Stability. Additional experiments explored the extent to which PDMS incorporation influenced the thermal stability

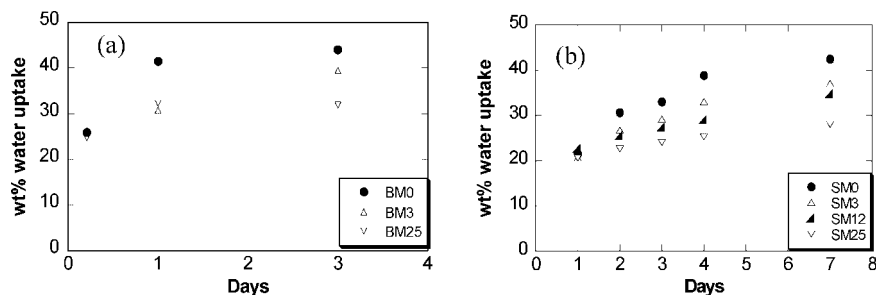


Figure 9. PDMS content effect on water uptake in (a) batch polymerization and (b) semicontinuous polymerization (miniemulsion feeding).

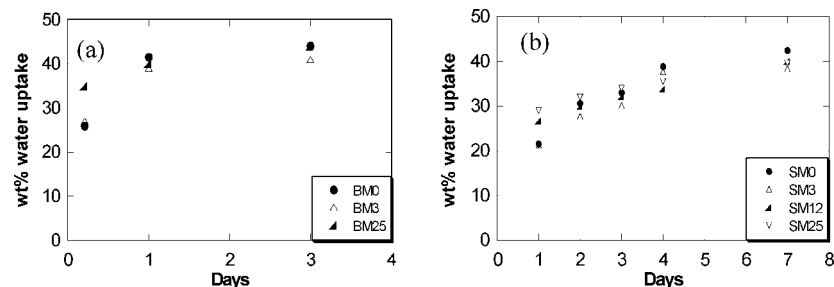


Figure 10. Water uptake normalized to the acrylic polymer content as a function of water immersion time for coatings from hybrid latex prepared by (a) batch polymerization and (b) semicontinuous polymerization (miniemulsion feeding), for increasing PDMS concentrations as indicated in the legend.

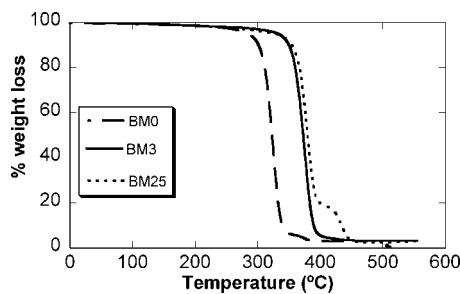


Figure 11. Representative TGA thermograms for batch method hybrid latex coatings with increasing PDMS content, as indicated in the legend.

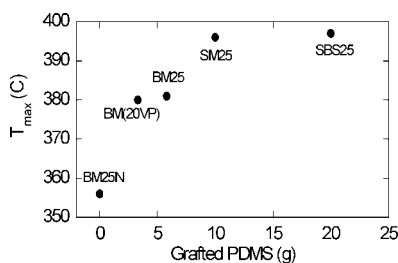


Figure 12. Effect of amount of grafted PDMS on thermal stability (represented as the temperature having the maximum rate of weight loss (T_{max})) of coatings containing the same amount of PDMS (25 g/100 g of acrylic copolymer).

of the hybrid coatings. Figure 11 compares the thermograms obtained from thermogravimetric analysis of the latexes produced in batch. This figure shows that an increase in the amount of PDMS leads to an increase in the temperature at which the material decomposes. The lowest decomposition temperature is seen for the acrylic latex without any PDMS (BM0), and the other two latexes containing PDMS have a higher decomposition temperature. Comparing BM3 and BM25, it is apparent that the decomposition temperature increases as the PDMS content increases. In addition, it was also observed that the latex containing 25 wt % PDMS showed a second decomposition

temperature at ≈ 450 °C. This second event is attributed to the decomposition of the nonreacted PDMS fraction, as it corresponds to our experimentally observed onset of thermal decomposition in the neat PDMS and also agrees with the literature value.²⁵

Further experiments found the thermal stability to depend also on the extent of silicone grafting to the acrylic, in addition to the total amount in the hybrid. Figure 12 shows that as the amount of grafted PDMS increases, the decomposition temperature likewise increases. The decomposition temperature, T_{max} , was defined as the temperature at which the rate of weight loss (due to the acrylic decomposition) was at a maximum. The various methods of polymerization are thus seen to have a pronounced impact on the thermal stability of the coating. To be effective in imparting thermal stability, the silicone must be grafted to the acrylic. The greatest amount of grafting, and hence the greatest thermal stability, was achieved by the semicontinuous method of emulsion polymerization.

Conclusions

High-solids silicone–acrylic hybrid latexes were produced by miniemulsion polymerization. The extent of the PDMS grafting to the acrylic copolymer was varied by using different PDMS (divinyl terminated, DV-PDMS; monovinyl terminated, MV-PDMS; and nonreactive, N-PDMS) and polymerization processes (batch and two different semicontinuous strategies).

It was found that PDMS incorporation followed this order: DV-PDMS > MV-PDMS > N-PDMS. The semicontinuous method (denoted as SM) led to a higher incorporation of the PDMS compared to the batch method (BM). Moreover, a delayed addition of the monomer during the semicontinuous process (denoted as SBS) resulted in an increase in the PDMS incorporation.

Blends of a PDMS emulsion with the acrylic latex were found to exhibit nonuniform drying in the vertical direction. At later drying times, the water loss rate was significantly slower than what was observed in the hybrid latex (SM25), and the total time for water loss was much longer. The data for the blends of PDMS and acrylic can be explained by silicone droplets partially coalescing near the film surface to create a skin layer

that impedes water loss. A clear advantage of the hybrid latex is that there is faster and more uniform drying, because the PDMS coalescence and consequent skin formation are avoided. Furthermore, it was found that PDMS was uniformly distributed throughout the film, at least within the resolution of the MR profiling technique. No evidence for PDMS migration upon heating was observed, indicating that the hybrid structure is robust.

For the batch latex coatings, the water contact angle substantially increased up to 5% PDMS (on the acrylic copolymer). Further increases of the PDMS content only led to marginal increases of the contact angle, probably because most of the additional PDMS was localized in the core of the particles. The higher incorporation of PDMS achieved with the semicontinuous processes led to higher contact angles. For coatings containing the same amount of PDMS, there was a clear correlation between the amount of PDMS grafted to the acrylic and the water contact angle. The water uptake of the acrylic part of the polymer was only slightly affected by the presence of PDMS. In coatings containing the same total amount of PDMS, the thermal stability significantly increased with the amount of PDMS grafted to the acrylic chains, regardless of the total amount of PDMS. Therefore, to achieve hydrophobic coatings with high thermal stability, the silicone must be chemically grafted to the acrylic and not merely included in the formulation. With a silicone core/acrylic shell particle structure, the encapsulated silicone phase cannot contribute significantly to the coating's hydrophobicity nor to its thermal stability. These properties are only affected when the silicone is incorporated into the acrylic at the molecular level.

Acknowledgment. Financial support from MEC (MAT 2003-01963) and Diputación Foral de Gipuzkoa is greatly appreciated. Funding for P.E. and C.H.A. was provided by the European Commission's Sixth Framework Programme through the NAPOLEON Project (Contract No. IP 011844-2). We thank A. Valori (University of Surrey) for assistance with the T_2 relaxation time measurements. We thank A. M. König and D. Johannsmann (Clausthal University of Technology) for useful comments and for

writing a computer program to assist with the GARField data analysis.

References and Notes

- (1) Daniel, J. C. In *Les Latex Synthétiques, Élaboration, Propriétés, Applications*; Daniel, J. C., Pichot C., Eds.; Lavoisier: Paris, 2006; p 319.
- (2) Lin, M.; Chu, F.; Guyot, A.; Putaux, J. L.; Bourgeat-Lami, E. *Polymer* **2005**, *46*, 1331–1337.
- (3) Kan, C. Y.; Kong, X. Z.; Yuan, Q.; Liu, D. S. *J. Appl. Polym. Sci.* **2001**, *80*, 2251–2258.
- (4) Kan, C. Y.; Liu, D. S.; Kong, X. Z.; Zhu, X. *J. Appl. Polym. Sci.* **2001**, *82*, 3194–3200.
- (5) Yuan, J.; Gu, G.; Zhou, S.; Wu, L. *High Perform. Polym.* **2004**, *16*, 69–80.
- (6) Liu, J.; Chen, L. Q.; Lei, W.; Zhang, L. M. *J. Macromol. Sci.* **2004**, *A41*, 913–925.
- (7) Asua, J. M. *Prog. Polym. Sci.* **2002**, *27*, 1283–1346.
- (8) Marcu, I.; Daniels, E. C.; Dimonie, V. L.; Roberts, J. E.; El-Aasser, M. S. *Prog. Colloid Polym. Sci.* **2003**, *124*, 31–36.
- (9) Yu, Z. Q.; Ni, P. H.; Li, J. A.; Zhu, X. L. *Colloids Surf., A: Physicochem. Eng. Aspects* **2004**, *242*, 9–15.
- (10) Mallégol, J.; Bennett, G.; McDonald, P. J.; Keddie, J. L.; Dupont, O. *J. Adhes.* **2006**, *82*, 217–238.
- (11) Routh, A. F.; Russel, W. B. *Langmuir* **1999**, *15*, 7762–7773.
- (12) Erkselius, S.; Wadsö, L.; Karlsson, O. J. *J. Colloid Interface Sci.* **2008**, *317*, 83–95.
- (13) Agarwal, A.; Farris, R. J. *J. Appl. Polym. Sci.* **1999**, *72*, 1407–1419.
- (14) Guigner, D.; Fischer, C.; Holl, Y. *Langmuir* **2001**, *17*, 3598–3606.
- (15) Glover, P. M.; Aptaker, P. S.; Bowler, J. R.; Ciampi, E.; McDonald, P. J. *J. Magn. Reson.* **1999**, *139*, 90–97.
- (16) Bennet, G.; Gorce, J. P.; Keddie, J. L.; McDonald, P. J.; Berglund, H. *Magn. Reson. Imaging* **2003**, *21*, 235–241.
- (17) Gorce, J. P.; Bovey, D.; McDonald, P. J.; Palasz, P.; Taylor, D.; Keddie, J. L. *Eur. Phys. J.* **2002**, *8*, 421–429.
- (18) McDonald, P. J.; Newling, B. *Rep. Prog. Phys.* **1998**, *61*, 1441–1492.
- (19) Narita, T.; Hebraud, P.; Lequeux, F. *Eur. Phys. J., E* **2005**, *17*, 69–76.
- (20) König, A. M.; Weerakkody, T. G.; Keddie, J. L.; Johannsmann, D. *Langmuir* **2008**, *24*, 7580–7589.
- (21) Routh, A. F.; Russel, W. B. *Ind. Chem. Res.* **2001**, *40*, 4302–4308.
- (22) Scott, W. W.; Bhushan, B. *Ultramicroscopy* **2003**, *97*, 151–169.
- (23) Aramendia, E.; Mallégol, J.; Jeynes, C.; Barandiaran, M. J.; Keddie, J. L.; Asua, J. M. *Langmuir* **2003**, *19*, 3212–3221.
- (24) Hergeth, W. D. Private communication.
- (25) Deshpande, G.; Rezac, M. E. *Polym. Degrad. Stab.* **2002**, *76*, 17–24.

MA8006015